Front. Struct. Civ. Eng. 2018, 12(3): 412–424
https://doi.org/10.1007/s11709-017-0432-8

RESEARCH ARTICLE

Application of a weakly compressible smoothed particle hydrodynamics multi-phase model to non-cohesive embankment breaching due to flow overtopping

Rasoul MEMARZADEH*, Gholamabbas BARANI, Mahnaz GHAEINI-HESSAROEYEH

Department of Civil Engineering, Faculty of Engineering, Shahid Bahonar University of Kerman, Kerman, Iran
**Corresponding author. E-mail: rasoul.memarzadeh@gmail.com*

ABSTRACT The subject of present study is the application of mesh free Lagrangian two-dimensional non-cohesive sediment transport model applied to a two-phase flow over an initially trapezoidal-shaped sediment embankment. The governing equations of the present model are the Navier-Stocks equations solved using Weakly Compressible Smoothed Particle Hydrodynamics (WCSPH) method. To simulate the movement of sediment particles, the model considers a powerful two-part technique; when the sediment phase has rigid behavior, only the force term due to shear stress in the Navier-Stokes equations is used for simulation of sediment particles' movement. Otherwise, all the Navier-Stokes force terms are used for transport simulation of sediment particles. In the present model, the interactions between different phases are calculated automatically, even with considerable difference between the density and viscosity of phases. Validation of the model is performed using simulation of available laboratory experiments, and the comparison between computational results and experimental data shows that the model generally predicts well the flow propagation over movable beds, the induced sediment transport and bed changes, and temporal evolution of embankment breaching.

KEYWORDS WCSPH method, non-cohesive sediment transport, rheological model, two-part technique, two-phase dam break

1 Introduction

Embankments and dikes along rivers are designed to protect cities and agricultural lands from floods. However, flooding of river valleys is an old concern and still a number of events occur yearly causing both monetary and human losses. Therefore, the study of embankment breaching is necessary to evaluate the damages due to overtopping floods. The numerical modeling has become a robust tool in the field of fluvial hydraulics and dike breaching in particular. The main difficulty in the study of embankment breaching process is the modeling of solid transport.

In the last few decades, many one-dimensional and two-dimensional numerical models have been developed to simulate the embankment breaching (e.g., [1–8]). Most of the existing breaching models are based on Finite Difference method and Finite Volume method. In these models, additional interface tracking schemes, such as volume of fluid, must be utilized which enabled them to handle the interfacial deformations.

In the present study, Smoothed Particle Hydrodynamics (SPH) method with sub-particle-scale large-eddy-simulation (SPS-LES) closure model is utilized to study the embankment breaching process. SPH is a mesh-free Lagrangian method originally developed for astrophysics modeling [9,10]. In this method, the weighted averaging process is used to approximate derivatives and physical properties. The SPH method has been used to study a variety of flow problems such as water wave impacts on coastal and offshore structures (e.g., [11]), flow over spillways (e.g., [12]), waves (e.g., [13–16]), groundwater flows and stability of levees (e.g., [17]), multi-phase flows for coastal and other hydraulic applications with air water mixtures and sediment scouring (e.g., [18–22]) and high velocity impact [23]. Furthermore, SPH method with

Article history: Received Jan 3, 2017; Accepted Apr 12, 2017

various solution algorithms is used successfully to model the fixed-bed dam break flow on a dry-bed and wet-bed downstream channel (e.g., [24–30]). The possibility of correctly simulating free surface and interface between different phases with various properties was a key factor for developing an embankment erosion model based on the SPH method.

There are few studies, which use particle based methods for modeling of sediment transport, especially for the bed load transport under steady-state flows with open boundaries. In one of these studies, Shakibaeinia and Jin [31] developed a multi-phase model based on MPS method. They used a single set of equations to model dam break waves over mobile beds and a rheological model to calculate the viscosity of sediment phase. In the field of SPH method, Manenti et al. [19] developed a three-dimensional SPH model to simulate a flushing problem in an artificial reservoir which uses Mohr-Coulomb yielding criterion and Shields theory to describe the failure mechanism of bottom sediments. Ran et al. [21] developed a multi-phase SPH model based on the principle of pick-up flow velocity. Fourtakas and Rogers [32] developed Smoothed Particle Hydrodynamics (SPH) multi-phase model accelerated with a graphics processing unit (GPU) which uses the Drucker-Prager yield criterion to predict the yielding characteristics of the sediment surface and a suspension model based on the volumetric concentration of the sediment.

In the present paper, the water and sediment phases are considered as a weakly compressible fluid. The movement simulation of the sediment phase is performed using a two-part technique. In this approach, a strength threshold for sediment particles is defined. When this threshold is not exceeded, only the force due to the shear stress is considered to move the sediment particles while, when the hydrodynamic shear stress overcomes the threshold, the sediment is allowed to move according to the equations of motion of water phase. The Bingham non-Newtonian constitutive model is used to obtain the threshold between the rigid or pseudo fluid behavior of bed sediment particles. This viewpoint for simulation of sediment particles is the main novelty of present model.

To assess the present model, first the present model is applied to a two-phase dam break problem based on the experimental data of Jánosi et al. [33]. Then, the embankment breaching process is studied using the experimental data of Schmocker and Hager [34]. Furthermore, additional tests are performed to study the influence of particle resolution on the numerical results.

2 Governing equations

It is hypothesized that the multi-phase system of embankment breaching problem can be considered as a multi-density multi-viscosity fluid. Therefore, the mass and momentum conservation equations are used to express the multi-phase system:

$$\frac{D\rho}{Dt} + \rho(\nabla \cdot \boldsymbol{u}) = 0, \tag{1}$$

$$\frac{D\boldsymbol{u}}{Dt} = -\frac{1}{\rho}\nabla P + \frac{\mu}{\rho}\left(\nabla^2 \boldsymbol{u}\right) + \boldsymbol{g}, \tag{2}$$

where ρ is the density, $\boldsymbol{u}$ is the flow velocity, P is the pressure, μ is the dynamic viscosity, $\boldsymbol{g}$ is gravitational acceleration vector and t is the time. The LES mass and momentum conservation equations for the particle scale flow are expressed as:

$$\frac{D\rho}{Dt} + \rho(\nabla \cdot \overline{\boldsymbol{u}}) = 0, \tag{3}$$

$$D\frac{\overline{\boldsymbol{u}}}{Dt} = -\frac{1}{\rho}\nabla \overline{p} + \frac{\mu}{\rho}(\nabla^2 \overline{\boldsymbol{u}}) + \boldsymbol{g} + \frac{1}{\rho}\nabla . \overline{\overline{\boldsymbol{\tau}}}, \tag{4}$$

where $'-'$ denotes the particle scale components, and $\overline{\overline{\boldsymbol{\tau}}}$ is the SPS stress tensor [35]. The motion of each particle is simply calculated by $\mathrm{D}\boldsymbol{r}/\mathrm{D}t = \overline{\boldsymbol{u}}$, with $\boldsymbol{r}$ being the position vector. To solve these equations SPH method is used for approximation of spatial derivatives. In the following equations, symbol $'-'$ is dropped for convenience.

3 SPH approximations

SPH method represents the continuum domain by discrete particles. The main idea of SPH method is to follow the particles in their motion. The particles can be considered as the material points carrying the physical properties of it (e.g., mass and density) and quantities of flow (e.g., velocity and pressure). The SPH interpolation procedure is based on the position of particles using a Lagrangian kernel function [36]. For Lagrangian kernels, the neighbors of influence do not change during the course of the simulation, but the domain of influence in the current configuration changes with time [36]. The kernel (or weighting) function, W, depends on the distance between the central particle (i) and other particles in its vicinity (j), either in same phase or different phases, and smoothing length h controls the support domain around the central particle (In the present simulations $h = 1.2 \times dr$ are used, where dr is the initial particle spacing). In the present model, the following kernel based on the spline function is adopted [24]:

$$W = \begin{cases} \frac{10}{7\pi h^2}\left(1 - \frac{3}{2}\left(\frac{r}{h}\right)^2 + \frac{3}{4}\left(\frac{r}{h}\right)^3\right) & \text{if } 0 \leqslant \left(\frac{r}{h}\right) < 1 \\ \frac{10}{28\pi h^2}\left(2 - \left(\frac{r}{h}\right)\right)^3 & \text{if } 1 \leqslant \left(\frac{r}{h}\right) \leqslant 2 \\ 0 & \text{otherwise} \end{cases}. \tag{5}$$

A detailed explanation of the SPH theories can be found in [10]. By applying the SPH interpolation to the governing Eqs. (3) and (4), the following relations are obtained:

$$\left(\frac{D\rho}{Dt}\right)_i = \sum_j m_j(\boldsymbol{u}_j - \boldsymbol{u}_i).\nabla_i W_{ij}, \tag{6}$$

$$\begin{aligned}\left(\frac{Du}{Dt}\right)_i = &-\sum_j m_j\left(\frac{P_j}{\rho_j^2}+\frac{P_i}{\rho_i^2}\right).\nabla_i W_{ij} \\ &+\sum_j \frac{2m_j\left(\frac{\mu_i}{\rho_i}+\frac{\mu_j}{\rho_j}\right)r_{ij}.\nabla_i W_{ij}}{\left(\rho_i+\rho_j\right)(|r_{ij}|^2+(0.01h)^2)} \\ &\times(\boldsymbol{u}_i-\boldsymbol{u}_j)+\boldsymbol{g} \\ &+\sum_j m_j\left(\frac{\vec{\boldsymbol{\tau}}_j}{\rho_j^2}+\frac{\vec{\boldsymbol{\tau}}_i}{\rho_i^2}\right).\nabla_i W_{ij},\end{aligned} \tag{7}$$

where $\boldsymbol{r}_{ij} = \boldsymbol{r}_i - \boldsymbol{r}_j$ and m is the mass of particles.

4 Multi-phase model

According to the status of non-cohesive sediments of the embankment, they are modeled in two different ways. The main idea of this approach is representing the sediments as granular material through the Bingham non-Newtonian rheological model. The Bingham material has a strength threshold (τ_y); when the stresses exceed this threshold, it flows as a viscous fluid:

$$\tau = \begin{cases} \left(\frac{\tau_y}{\sqrt{II_E}}+2\mu_0\right)\boldsymbol{E} & |\tau|>\tau_y \\ 0 & |\tau|\leqslant\tau_y \end{cases}. \tag{8}$$

In which μ_0 is the flow consistency index depending on sediment mass density, sediment diameter and viscosity of the main fluid [37], and is constant during the computations; $\boldsymbol{E}$ is the strain rate tensor; and $II_{\boldsymbol{E}}$ is second principal invariant of the shear strain rate tensor:

$$\begin{aligned}\boldsymbol{E} &= \begin{pmatrix} \frac{\partial u}{\partial x} & \frac{1}{2}\left(\frac{\partial u}{\partial z}+\frac{\partial w}{\partial x}\right) \\ \frac{1}{2}\left(\frac{\partial u}{\partial z}+\frac{\partial w}{\partial x}\right) & \frac{\partial w}{\partial z} \end{pmatrix} \\ II_E &= 0.5\left(\frac{\partial u}{\partial x}\right)^2+0.5\left(\frac{\partial w}{\partial z}\right)^2+0.25\left(\frac{\partial w}{\partial z}+\frac{\partial u}{\partial z}\right)^2.\end{aligned} \tag{9}$$

The threshold strength or yield stress of non-cohesive sediment particles is defined by the following equation [38]:

$$\tau_y = \overline{\sigma}\sin\phi, \tag{10}$$

where ϕ is the internal friction angle of sediment and $\overline{\sigma}$ is the normal stress between the sediment grains.

In the present model, when the hydrodynamic shear stress on an interface grain induced by the flow overcomes its threshold strength (i.e., $\sqrt{II_E} > \frac{\tau_y}{2\alpha\mu_0}$ in which $\alpha = 100$), it is modeled as slightly compressible fluid whose dynamic viscosity is determined according the following equation:

$$\mu = \frac{\tau_y}{\sqrt{4II_E}}+\mu_0. \tag{11}$$

In this step, which sediment particles behave like the pseudo fluid, all terms of the momentum Eq. (4) are used to move the sediment particle. Otherwise, when the shear stress falls below the strength threshold, the particle is assumed to move under the influence of the shear stress force term of Eq. (4).

In the proposed model, the multi-phase forces between various phases are calculated automatically, even when there is a considerable difference between the density and viscosity of phases. In the present multi-phase model, based on the properties of SPH method, the domain of the problem represents as particles with various density and viscosity. The behavior of a particle, which interacting with other particles in its neighborhood, depends on its viscosity and density and viscosity and density of neighboring particles. In the interface layer between sediment and water phase, particles of same and another phase are used to discretize the equations of each phase particles. Thus, effect of difference phases automatically is applied to calculate the multi-phase forces for simulation of sediment (in both parts) and water phases. The consideration of density and viscosity differences in calculation of multi-phase forces can be seen in the Eq. (7). As a result, the solutions of separate equations for each phase and then calculations of the multi-phase forces are not required. As a result, the solutions of separate equations for each phase and calculations of the multi-phase forces are not required.

5 Solution algorithm

The system of equations is solved in two pseudo steps, adopting a fractional step approach (i.e., prediction and correction steps). For a new time step, the positions and velocities of water and sediment particles are computed by the following equations:

$$\boldsymbol{u}_{t+1} = \boldsymbol{u}_t + \boldsymbol{u}_* + \boldsymbol{u}_{**}, \tag{12}$$

$$\boldsymbol{r}_{t+1} = \boldsymbol{r}_t + \frac{\boldsymbol{u}_{t+1} + \boldsymbol{u}_t}{2}\Delta t, \tag{13}$$

where $\boldsymbol{u}_*$ and $\boldsymbol{u}_{**}$ are the calculated velocities in the prediction and correction steps. For the different types of particles, these velocity terms are calculated separately:

Water particles:

$$\boldsymbol{u}_* = ((\mu\nabla^2\boldsymbol{u}) + \nabla.\vec{\vec{\boldsymbol{\tau}}} + \boldsymbol{g})\Delta t, \tag{14}$$

$$\boldsymbol{u}_{**} = \left(\frac{-1}{\rho^*}\nabla P^{t+1}\right)\Delta t. \tag{15}$$

Sediment particles with rigid behavior (i.e., the particle whose shear stress on it does not exceed the yield stress):

$$\boldsymbol{u}_* = (\mu\nabla^2\boldsymbol{u} + \nabla.\vec{\vec{\boldsymbol{\tau}}})\Delta t, \tag{16}$$

$$\boldsymbol{u}_{**} = 0.0. \tag{17}$$

Sediment particles with pseudo viscous fluid behavior:

$$\boldsymbol{u}_* = ((\mu\nabla^2\boldsymbol{u}) + \boldsymbol{g})\Delta t, \tag{18}$$

$$\boldsymbol{u}_{**} = \left(\frac{-1}{\rho^*}\nabla P^{t+1}\right)\Delta t. \tag{19}$$

In the present paper, the weakly compressible SPH is used for the pressure calculation [39]. The water and sediment particles are assumed to be weakly compressible, and the Tait's state equation, an explicit equation, is used to calculate the pressures of particles in each time step [39]:

$$P_i^{t+1} = \frac{\rho_i^0 c_0^2}{\gamma}\left(\left(\frac{\rho_i^*}{\rho_i^0}\right)^{\gamma} - 1\right). \tag{20}$$

In which, $\gamma = 7$, c_0 is the numerical sound speed in reference density, ρ_i^0 is density of particle i in start of time step and ρ_i^* is density of particle i in prediction step. In addition, the solution algorithm is schematically shown in Fig. 1.

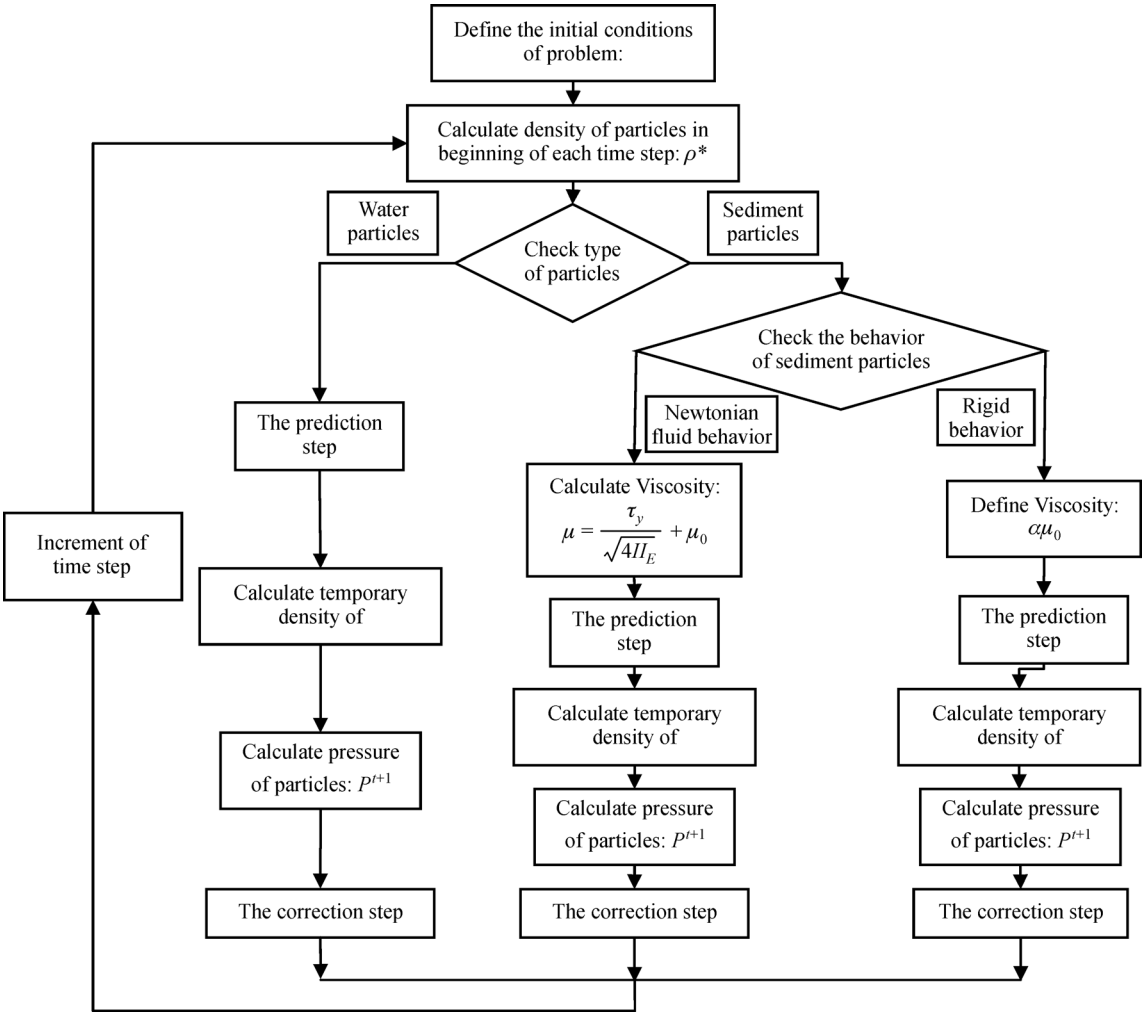

Fig. 1 Solution algorithm of WCSPH multi-phase model

6 Boundary conditions

Four kinds of boundary conditions are used to model the present study's problems: solid walls, free surface, inflow and outflow. Solid walls are described by one line of particles, and the velocities of wall particles are set zero to represent the non-slip boundary condition. Moreover, two lines of dummy particles are placed outside of wall boundaries in order to ensure that the densities of wall particles are computed accurately, and wall particles are not considered as free surface particles. The pressure of a dummy particle is set equal to wall particle pressure in the normal direction of the solid walls [24]. The particles which satisfy the following equation are considered as free surface particles and zero pressure is applied to them:

$$(\rho_*)_i < \beta \times (\rho_0)_i. \tag{21}$$

In this equation β is the free surface parameter and $0.9<\beta<0.99$ [24]. Inflow and outflow are modeled by motion of particles toward and outward of the solution domain based on the recycling strategy, which is represented by Shakibaeinia and Jin [40].

7 Model applications

The present model is applied to two laboratory tests. In the first section, the performance of the WCSPH multi-phase model is evaluated with two-phase (liquid–liquid) dam break. Then, the model is applied to plane embankment breaching problem.

7.1 Two-phase dam break

In this section, WCSPH multi-phase model will be applied to model two phase dam break problem. The initial geometry of problem is shown in Fig. 2. To validate the computations of WCSPH multi-phase model, the experimental data of Jánosi et al. [33] is used. In this experiment, the gate has been opened completely from above with a constant speed of 1.5 m/s. During the modeling, the total number of fluid particles are 21,068, corresponding to a particle spacing of 0.002 in the initial configuration. The fluid particles are initially arranged in a regular, equally-spaced grid, with 872 boundary particles add to form the left and right-hand wall and bed. In the computation a constant time step of 0.0002 s is employed. The density and dynamic viscosity of water are 1000 kg/m^3 and 10^{-6} m^2/s. The downstream channel contains the PEO (poly-ethylene-oxide) solutions with a concentration of 42 wppm and depth of 0.015 m. The viscosity of this solution is 0.935×10^{-6} m^2/s and density of it is close to density of water [33]. Both fluids (water and PEO solution) are considered as Newtonian fluids, and a constant viscosity is assigned.

The computational particle configurations for the flow after gate removal and experimental results of Jánosi et al. [33] at different times t = 0.131 s, 0.196 s, 0.261 s, 0.327 s and 0.392 s are shown in Fig. 3. The smooth shape of the free surface and the satisfactory agreement with the experimental results prove the accuracy of WCSPH multi-phase model. The small discrepancy is seen which can be the result of the extra dimension in the experiments and the effect of the gate roughness. Because of resting fluid in the channel tend to block the flow, the collision with the moving front results in an up thrust generating the mushroom jet. Furthermore, as can be seen in Fig. 3, the mixture process of water and PEO solution particles and interface layer between different phases are modeled well. The mixture process is the main factor of velocity reduction of dam break flow. The well calculated mixture process shows that the present model calculates the multi-phase forces with a good accuracy.

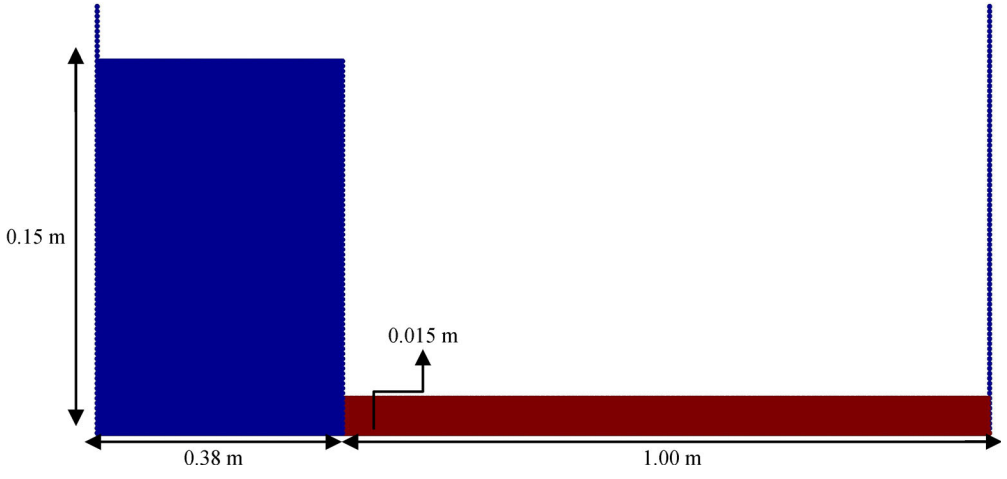

Fig. 2 Initial geometry of two-phase dam break problem

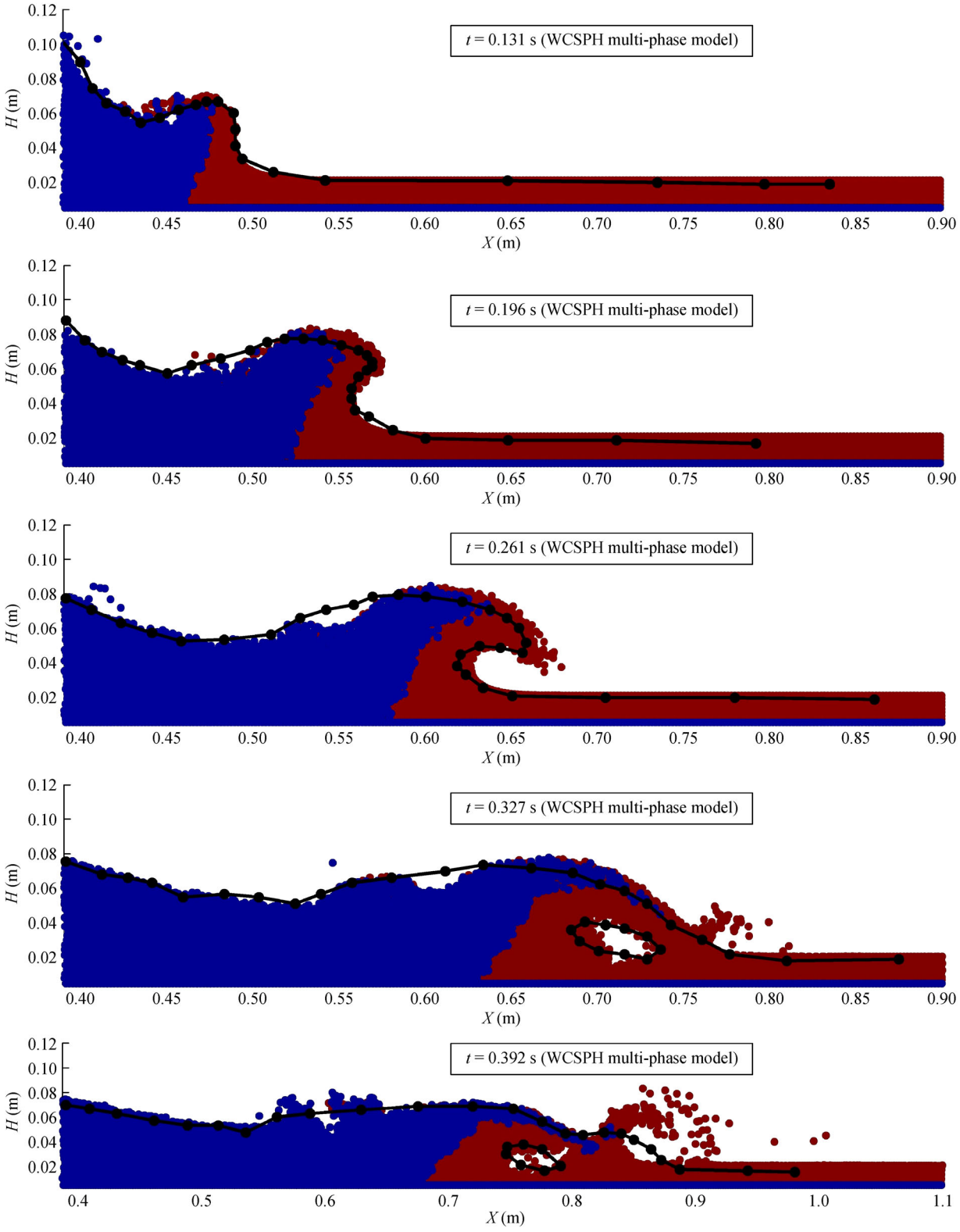

Fig. 3 Configurations of particles in different times after start of test, and comparisons between the free surface profile result of the WCSPH multi-phase model and experimental data of Jánosi et al. [33] (blue particles = water, red particles = PEO solution, black line = experimental data)

7.2 Plane embankment breach

In this section, the WCSPH multi-phase model is applied to model plane embankment breaching without lateral erosion based on the experimental data of Schmocker and Hager [34]. Schmocker and Hager [34] investigated the erosion of homogenous embankment due to flow overtopping. The test with the following parameters is selected herein: The embankment is inserted 1.0 m downstream from the intake. The height, width, crest length of embankment are $w = 0.2$ m, $b = 0.2$ m and $L_K = 0.1$ m. Up and downstream slopes are $S_0 = 1{:}2$ (V:H) and total embankment length is $L = 4w + L_K = 0.9$ m. The approach flow discharge is kept constant at $Q_0 = 11.31$ L/s. The embankment is built of non-cohesive dry sand of 2.0 mm in grain diameter with density $\rho = 2650$ kg/m^3 and angle of friction $\phi = 37°$. It is considered that the reservoir is initially empty, and it fills very fast in a few seconds. The initial particle spacing, dr, is 0.005 m. The average number of particles in the simulation is 21,000 particles.

In Fig. 4, the computational particle configurations at different times after the overtopping are shown. It is obvious from the figure that head cutting is the dominant mechanism in the beginning of the breaching process, and then the breaching gradually forms and expands. When the water flows through the downstream slope, the shear stresses in the flow field are formed, and the erosion process begins when this shear stress exceeds the resistive force in the bed soil. At the initial times of overtopping, the minor sediment erosion is occurred resulted from the small overflow discharge transporting sediment downstream. With the passage of time, by increasing the overflow discharge and velocity of flow, the high stress intensities are formed leading to an increase in the erosion rate. Overflow discharge erodes the downstream face of the embankment with a slope in parallel with it, and then progressively flattens this to a terminal value. These results are in agreement with the erosion process described by Coleman et al. [41].

The comparison between the computed bed evolution profiles by WCSPH multi-phase model and experimental data are shown in Fig. 5 at four different times after the overtopping being started, i.e., $t = 2.8$ s, 5.7 s, 8.5 s, and 14.1 s. The breach developments in the present computational modeling present promising agreements with the experimental data. In both numerical results and experiments, the embankment breaching process is initiated from the crest of embankment. Different from the measured

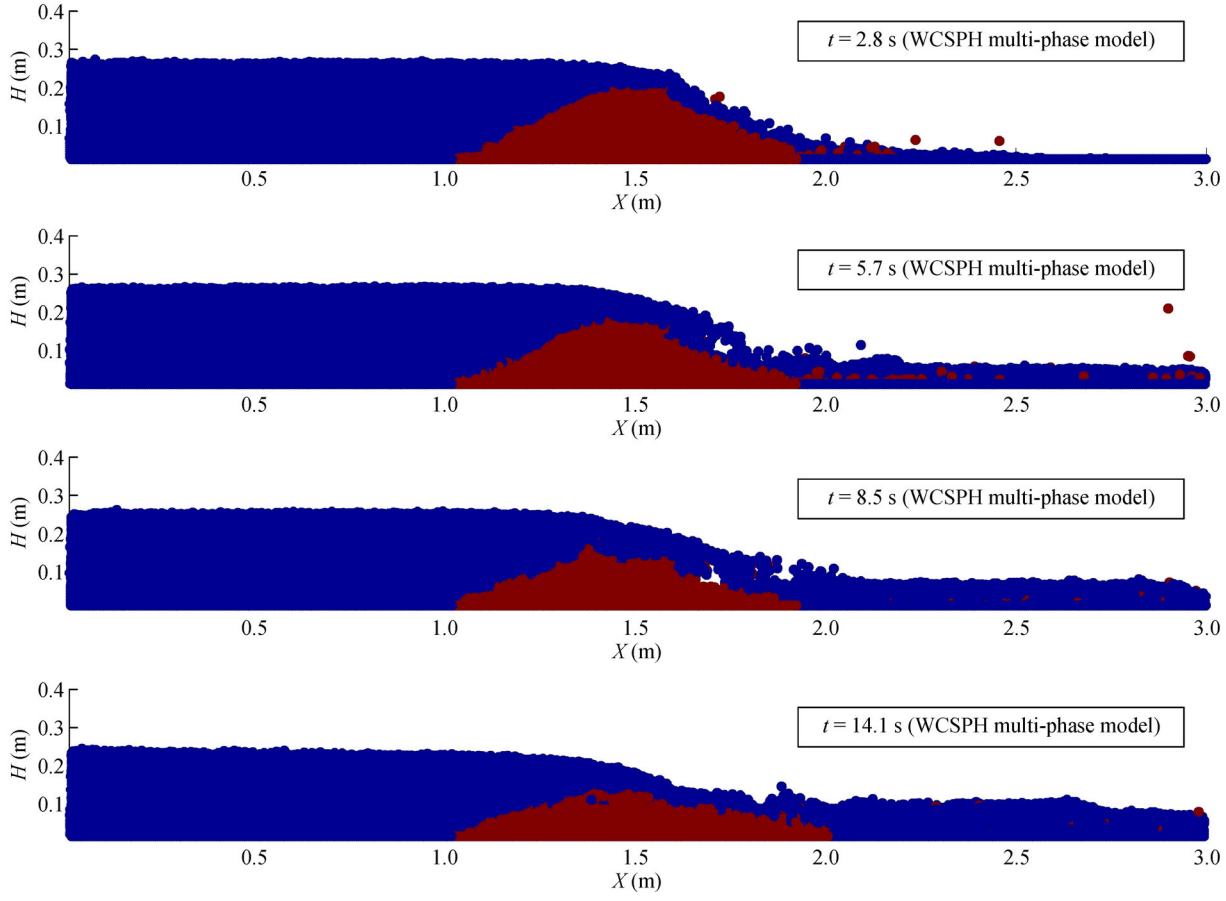

Fig. 4 Configurations of particles in different times after overtopping computed by WCSPH multi-phase model (Blue particles = water, brown particles = sediment, horizontal and vertical units are in meters)

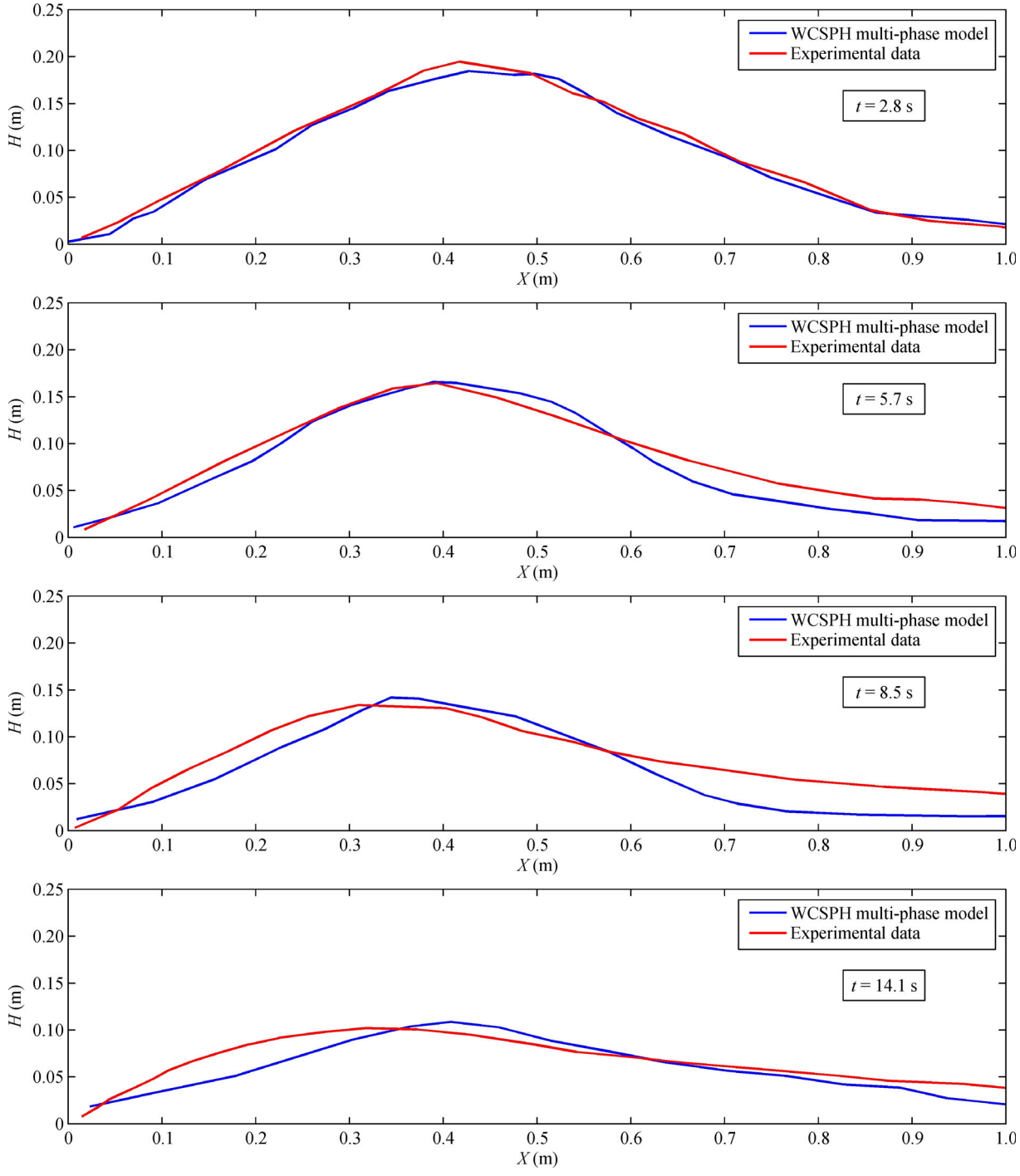

Fig. 5 Comparison of longitudinal embankment profile of WCSPH multi-phase model results and experimental data of Schmocker and Hager [34] at various times

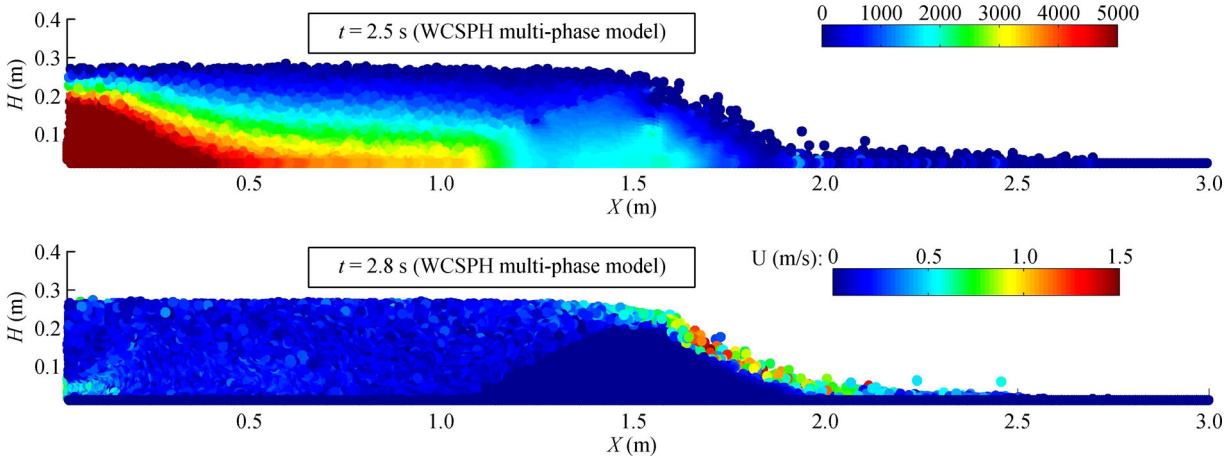

Fig. 6 Pressure and velocity field of embankment breaching problem computed by WCSPH multi-phase model (Unit of pressure and velocity is Pascal and m/s)

data, the small deposition of sediments occurred in the downstream of embankment in the numerical simulations. Along with the overtopping flow, these eroded sediment particles are removed from the computational domain. As can be seen in Fig. 5, the overall agreements between the computed and measured data are acceptable. Moreover, the satisfactory agreement between the modeled and experimental bed profiles shows that the WCSPH multi-phase model successfully reproduced the behavior of the sediment phase.

Figure 6 illustrates a snapshot of pressure and velocity field. As it has been shown, the model reproduces a relatively smooth pressure and velocity field, even near the sediment–water interface, although some small fluctuation in the pressure field is visible. This can be due the SPH unphysical fluctuations. Generally, the result appropriately illustrates the ability of the present model to simulate the flow features and the mixing process in embankment breaching.

Furthermore, the model convergence study is performed to demonstrate the sensitivity of model results on the particle spacing and evaluate the convergence of model. For this purpose, the computations are done with three particle spacing including $dr = 0.01$ m, 0.005 m, 0.0025 m. In the computations, the time steps are also proportionally reduced to be consistent with the decrease in particle spacing. In Fig. 7, the quantified comparison of the model results with different particle resolution and experimental data of Schmocker and Hager [34] is presented at selected times t = 2.8 s, 5.7 s, and 14.1 s. Also, an approximate calculated error between the results of WCSPH multi-phase model and experimental data is shown in Table 1. The comparisons have demonstrated that the error norms consistently decrease when the particle sizes become smaller. Also, refined simulations provide better agreement with the experimental data, indicating the convergence of the WCSPH multi-phase model.

7.2.1 Effect of flow condition on the breaching process

Two test cases are used to evaluate the effects of the flow conditions (i.e., flow discharge) on the breaching process. In these tests, the approach flow discharge are $Q_0 = 15$ l/s and $Q_0 = 20$ l/s. The results are shown in Fig. 8 and compared with the results of $Q_0 = 11$ l/s. The comparison shows that the flow discharge has the direct effect on the breaching process of embankment. With higher discharge, where the momentum of flow is high, the erosion process is developed faster, and the trapezoidal shape of embankment turns into a round-crested breach shape more quickly.

7.2.2 Effect of rheological properties on the breaching process

The rheological properties assigned to the sediments play an important role in the breaching process. In the Bingham Plastic model, the main rheological parameters are the consistency index (μ_0) and the friction angle (ϕ). Based on the properties of the embankment material [34], $\mu_0 =$ 0.6 pa·s and $\phi = 37°$ are used in the model (case 1). In this section, to investigate the effect of rheological properties, the model is implemented with varying rheological properties. In Fig. 9, the results of two different cases are compared with the results of case 1. In one of these cases, consistency index is 0.6 pa·s but without yield stress, i.e., $\phi = 0°$ (case 2). This condition is similar to a viscous Newtonian fluid. In another case, μ_0 is 0.06 pa·s and ϕ is

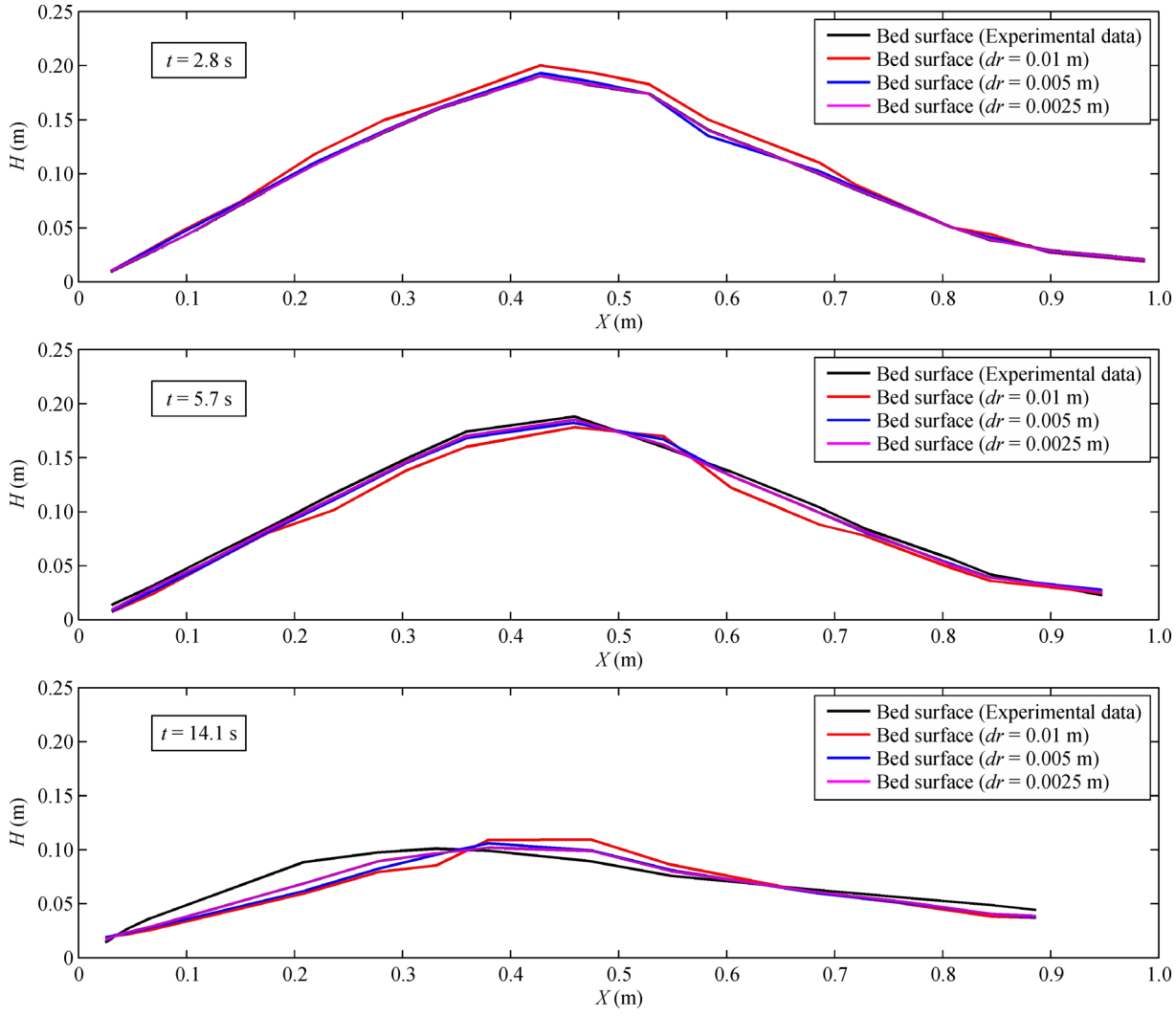

Fig. 7 Comparison of the present model results with different initial particle spacing with the experimental data of Schmocker and Hager [34]

Table 1 The approximate average error between numerical results with different particle spacing and experimental data of Schmocker and Hager [34]

time (s)	approximate average error (%)		
	$dr = 0.01$ m	$dr = 0.005$ m	$dr = 0.0025$ m
2.8	8.31	5.76	3.53
5.7	12.23	9.26	6.72
14.1	15.42	11.31	9.58

35° (case 3). The comparison shows when the sediment phase acts as a Newtonian fluid by setting the friction angle $\phi = 0°$, leads to a faster breaching process. Furthermore, reducing the consistency index reduces the erosion area of the embankment.

8 Conclusions

A two-dimensional WCSPH multi-phase model is presented to simulate the progressive erosion of non-cohesive embankments due to flow overtopping. SPH method is the

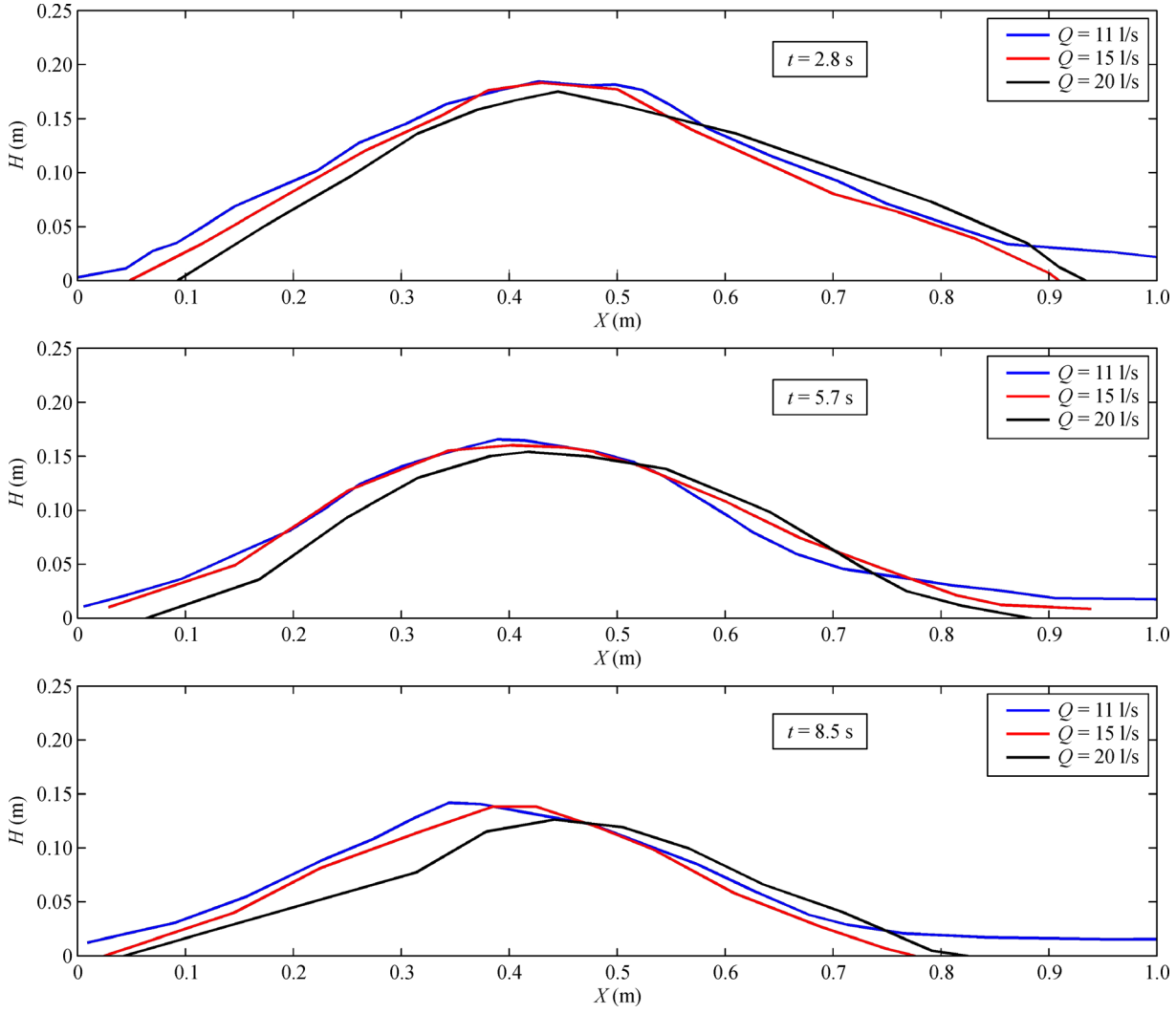

Fig. 8 Comparisons of longitudinal embankment profiles of WCSPH multi-phase results for different flow discharges at various times

one of the most famous particle methods which originally developed for astrophysical computations and later has been extended to a wide range of fluid mechanics problems. A two-part technique is developed which simulates the motion of sediment particles based on their behavior. In this technique, when the sediment phase behaves like the rigid material, only the force term due to shear stress is used for simulation of sediment particles' movement. Otherwise, all the Navier-Stokes force terms are used for transport simulation of sediment particles. Furthermore, the incorporated LES based SPS turbulence model using the Smagorinsky eddy viscosity is utilized to investigate the effects of turbulence. The numerical model is applied to two laboratory tests concerning multi-phase dam break flow and breaching of plane embankment. The numerical simulations prove that the overall results agree well with the experimental data, reproducing the main features of flows including turbulence, mixing process, interface fragmentations and scouring. In the case of multi-phase dam break flow, the free surface of flow and interface between different phases are modeled with satisfactory accuracy. In the plane embankment breach, scouring process is considered well. The use of two-part approach appears be appropriate for simulation of bed load transport under flows with high deformation. The alternative computations using three different particle spacing are performed to verify the convergence of the numerical scheme. Furthermore, the effects of the flow conditions and rheological behavior on the breaching process are investigated. The results show that the breaching process is performed faster when the flow discharge is higher, the sediment particles are considered as a Newtonian fluid and the consistency index of sediment particles are reduced. The reasonable agreement hereby confirms the applicability of present model to simulate the wide range of multi-phase flows.

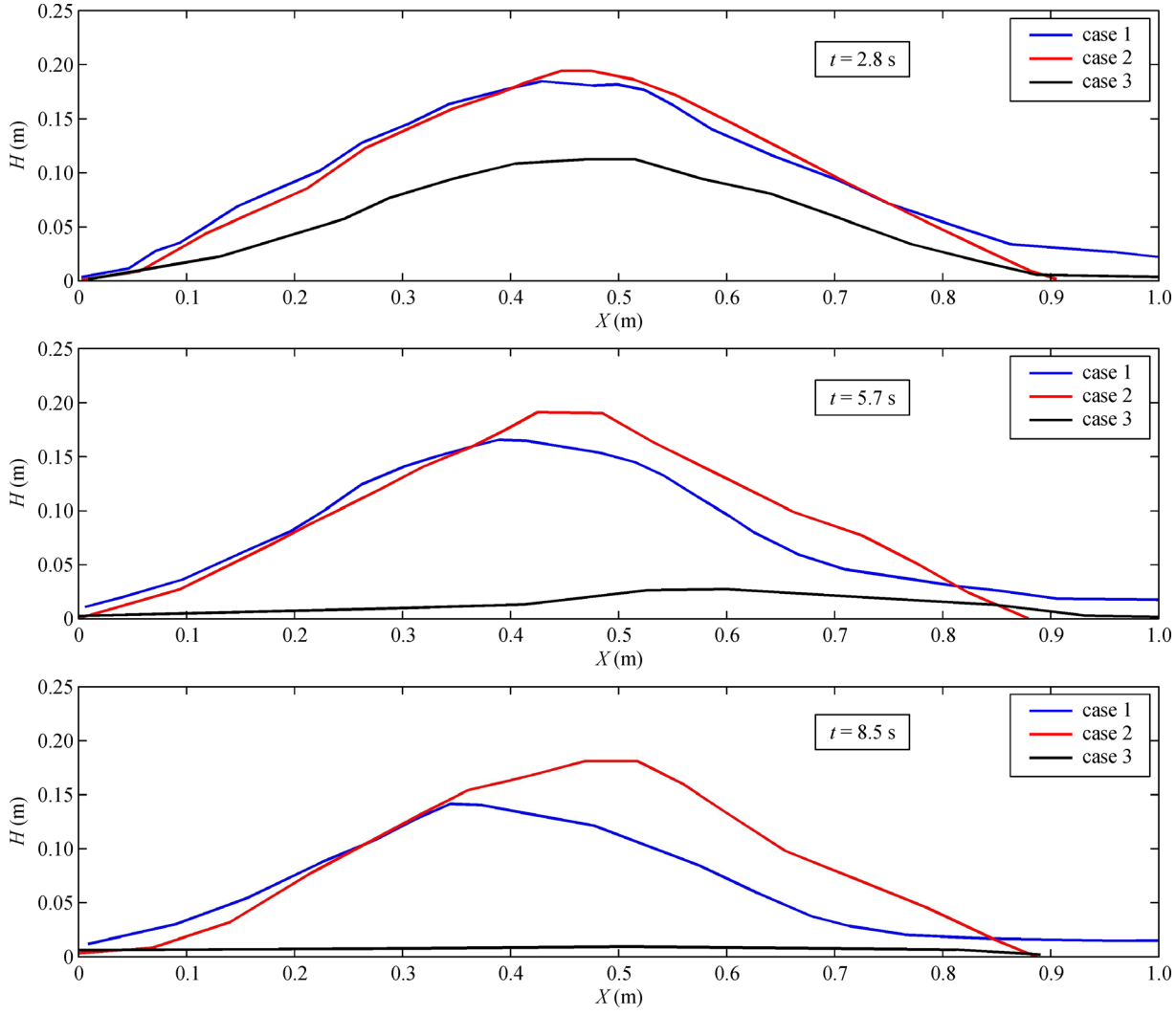

Fig. 9 Comparisons of longitudinal embankment profiles of WCSPH results for different rheological parameters at various times

References

1. Basco D R, Shin C S. A one-dimensional numerical model for storm-breaching of barrier islands. Journal of Coastal Research, 1999, 15(1): 241–260
2. Tingsanchali T, Chinnarasri C. Numerical modeling of dam failure due to flow overtopping. Hydrological Sciences Journal, 2001, 46 (1): 113–130
3. Wang Z, Bowles D S. Three-dimensional non-cohesive earthen dam breach model. Part 1: theory and methodology. Advances in Water Resources, 2006, 29(10): 1528–1545
4. Faeh R. Numerical modeling of breach erosion of river embankments. Journal of Hydraulic Engineering, 2007, 133(9): 1000–1009
5. Pontillo M, Schmocker L, Greco M, Hager W H. 1D numerical evaluation of dike erosion due to overtopping. Journal of Hydraulic Research, 2010, 48(5): 573–582
6. Volz C, Rousselot P, Vetsch D, Faeh R. Numerical modelling of non-cohesive embankment breach with the dual-mesh approach. Journal of Hydraulic Research, 2012, 50(6): 587–598
7. Wu W, Marsooli R, He Z. Depth-averaged two-dimensional model of unsteady flow and sediment transport due to noncohesive embankment break/breaching. Journal of Hydraulic Engineering, 2012, 138(6): 503–516
8. Kuiry S N, Ding Y, Wang S S Y. Numerical simulations of morphological changes in barrier islands induced by storm surges and waves using a supercritical flow model. Frontiers of Structural and Civil Engineering, 2014, 8(1): 57–68
9. Lucy L B. A numerical approach to the testing of the fission hypothesis. Astronomical Journal, 1977, 82(12): 1013–1024
10. Monaghan J J. Smoothed particle hydrodynamics. Annual Review of Astronomy and Astrophysics, 1992, 30(1): 543–574
11. Altomare C, Crespo A J C, Domínguez J M, Gómez-Gesteira M, Suzuki T, Verwaest T. Applicability of smoothed particle hydrodynamics for estimation of sea wave impact on coastal structures. Coastal Engineering, 2015, 96: 1–12
12. Husain S M, Muhammed J R, Karunarathna H U, Reeve D E. Investigation of pressure variations over stepped spillways using

smooth particle hydrodynamics. Advances in Water Resources, 2014, 66: 52–69
13. Ataie-Ashtiani B, Shobeyri G. Numerical simulation of landslide impulsive waves by incompressible smoothed particle hydrodynamics. International Journal for Numerical Methods in Fluids, 2008, 56(2): 209–232
14. Capone T, Panizzo A, Monaghan J J. SPH modelling of water waves generated by submarine landslides. Journal of Hydraulic Research, 2010, 48(sup1): 80–84
15. Memarzadeh R, Hejazi K. ISPH numerical modeling of nonlinear wave run-up on steep slopes. Journal of the Persian Gulf (Marine Science), 2012, 3(10): 17–26
16. Vacondio R, Rogers B D, Stansby P K, Mignosa P. Shallow water SPH for flooding with dynamic particle coalescing and splitting. Advances in Water Resources, 2013, 58: 10–23
17. Bui H H, Fukagawa R. An improved SPH method for saturated soils and its application to investigate the mechanisms of embankment failure: case of hydrostatic pore-water pressure. International Journal for Numerical and Analytical Methods in Geomechanics, 2013, 37(1): 31–50
18. Hosseini S M, Manzari M T, Hannani S K. A fully explicit three-step SPH algorithm for simulation of non-Newtonian fluid flow. International Journal of Numerical Methods for Heat & Fluid Flow, 2007, 17(7): 715–735
19. Manenti S, Sibilla S, Gallati M, Agate G, Guandalini R. SPH simulation of sediment flushing induced by a rapid water flow. Journal of Hydraulic Engineering, 2012, 138(3): 272–284
20. Razavitoosi S L, Ayyoubzadeh S A, Valizadeh A. Two-phase SPH modelling of waves caused by dam break over a movable bed. International Journal of Sediment Research, 2014, 29(3): 344–356
21. Ran Q, Tong J, Shao S, Fu X, Xu Y. Incompressible SPH scour model for movable bed dam break flows. Advances in Water Resources, 2015, 82: 39–50
22. Memarzadeh R, Barani G, Ghaeini-Hessaroeyeh M. Numerical modeling of sediment transport based on unsteady and steady flows by incompressible smoothed particle hydrodynamics method. Journal of Hydrodynamics, 2017, (in press)
23. Asadi Kalameh H, Karamali A, Anitescu C, Rabczuk T. High velocity impact of metal sphere on thin metallic plate using smooth particle hydrodynamics (SPH) method. Frontiers of Structural and Civil Engineering, 2012, 6(2): 101–110
24. Shao S, Lo E. Incompressible SPH method for simulating Newtonian and non Newtonian flows with a free surface. Advances in Water Resources, 2003, 26(7): 787–800
25. Ata R, Soulaimani A. A stabilized SPH method for inviscid shallow water flows. International Journal for Numerical Methods in Fluids, 2005, 47(2): 139–159
26. Crespo A J C, Gómez-Gesteira M, Dalrymple R A. Modeling dam break behavior over a wet bed by a SPH technique. Journal of Hydraulic Engineering, 2008, 134(6): 313–320
27. Lee E S, Moulinec C, Xu R, Violeau D, Laurence D, Stansby P. Comparisons of weakly compressible and truly incompressible algorithms for the SPH mesh free particle method. Journal of Computational Physics, 2008, 227(18): 8417–8436
28. Khayyer A, Gotoh H. On particle-based simulation of a dam break over a wet bed. Journal of Hydraulic Research, 2010, 48(2): 238–249
29. Ferrari A, Fraccarollo L, Dumbser M, Toro E F, Armanini A. Three-dimensional flow evolution after a dam break. Journal of Fluid Mechanics, 2010, 663: 456–477
30. Chang T J, Kao H M, Chang K H, Hsu M H. Numerical simulation of shallow-water dam break flows in open channels using smoothed particle hydrodynamics. Journal of Hydrology (Amsterdam), 2011, 408(1–2): 78–90
31. Shakibaeinia A, Jin Y C. A weakly compressible MPS method for modeling of open-boundary free-surface flow. International Journal for Numerical Methods in Fluids, 2010, 63(10): 1208–1232
32. Fourtakas G, Rogers B D. Modelling multi-phase liquid-sediment scour and resuspension induced by rapid flows using Smoothed Particle Hydrodynamics (SPH) accelerated with a Graphics Processing Unit (GPU). Advances in Water Resources, 2016, 92: 186–199
33. Jánosi I M, Jan D, Szabó K G, Tél T. Turbulent drag reduction in dam-break flows. Experiments in Fluids, 2004, 37(2): 219–229
34. Schmocker L, Hager W H. Modelling dike breaching due to overtopping. Journal of Hydraulic Research, 2009, 47(5): 585–597
35. Lo E Y M, Gotoh H, Shao S D. Simulation of near-shore solitary wave mechanics by an incompressible SPH method. Applied Ocean Research, 2002, 24(5): 275–286
36. Rabczuk T, Belytschko T, Xiao S P. Stable particle methods based on Lagrangian kernels. Computer Methods in Applied Mechanics and Engineering, 2004, 193(12–14): 1035–1063
37. Chen C L, Ling C H. Granular-flow rheology: role of shear-rate number in transition regime. Journal of Engineering Mechanics, 1996, 122(5): 469–480
38. Ken-Ichi K. A plasticity theory for the kinematics of ideal granular materials. International Journal of Engineering Science, 1982, 20 (1): 1–13
39. Monaghan J J. Simulating free surface flows with SPH. Journal of Computational Physics, 1994, 110(2): 399–406
40. Shakibaeinia A, Jin Y C. A mesh-free particle model for simulation of mobile-bed dam break. Advances in Water Resources, 2011, 34 (6): 794–807
41. Coleman S E, Andrews D P, Webby M G. Overtopping breaching of noncohesive homogeneous embankments. Journal of Hydraulic Engineering, 2002, 128(9): 829–838